STUDYING THE VARIATIONS IN AEROSOL LOADING AND THERMAL REGIME OF THE STRATOSPHERE OVER TOMSK ON THE BASIS OF LIDAR MONITORING

G.G. Matvienko, V.N. Marichev, D.A. Bochkovsky

V.E. Zuev Institute of Atmospheric Optics, Siberian Branch of the Russian Academy of Sciences,

Academician Zuev Square, Tomsk 634021, Russia, E-mail: mgg@iao.ru

ABSTRACT
One of the important applications of lidar techniques is the study of aerosol content and thermal regime of the stratosphere. Such investigations in monitoring mode were initiated at the Institute of Atmospheric Optics since 1986 (for aerosol) and 1994 (for temperature), and are continued to the present. The main attention is paid to studying the annual variations in aerosol content in the stratosphere and sudden disturbances caused by winter stratospheric warming. In this paper we present the results of studying the aerosol content and its vertical stratification and vertical distribution of temperature in the stratosphere over Tomsk for the last three years.

1 INTRODUCTION

The period of 2016-18, which presents the results was characterized by the absence of volcanic eruptions which could affect the disturbance of the aerosol component of the stratosphere of the northern hemisphere including western Siberian region. So it was a convenient possibility to observe the peculiarities of the temporal variability of the background aerosol loading of the stratosphere over Western Siberia during quite long time interval. In this period, as in previous years, winter stratospheric warming's were observed. This gave the opportunity to continue to study the peculiarities of their manifestations.
The represented data array of 222 total signals collected in some nights was used as initial data for analysis in 2016-18.The height interval was from 15 till 50-60 km, the spatial resolution was 192 m. Lidar signals were received in the photopulses counting mode with accumulation of по 12×10^4 laser pulses (accumulation time was about 2 hours during a night).

2 METHODOLOGY

Lidar methods of the Raman and elastic aerosol and molecular scattering of light (Raman, Mie and Rayleigh scattering) were used to determine the vertical profile of aerosol characteristics and temperature in the stratosphere. The atmospheric sounding was carried out by laser radiation at a wavelength of 532nm, the reception of the lidar signals at wavelengths 532 and 607 nm. The optical characteristics of the scattering ratio R(H) and the integral aerosol backscattering coefficient B(H) were used to estimate the aerosol filling of the stratosphere.
R(H) (H is the current height) describes the aerosol vertical stratification. By definition, R(H) is the ratio of the sum of aerosol and molecular backscattering coefficient to the molecular backscattering coefficient. For example, fulfillment of the condition R(H) = 1 means the absence of aerosol at the certain height, and contrary, aerosol appears where R(H) > 1. B (H) describes the temporal dynamics of the aerosol filling of the stratosphere according to the formula

$$B = \int_{H_1}^{H_2} \beta(h)dh$$

where *β(h)*- aerosol backscattering coefficient, H_1 is the height of the tropopause, and H_2 is chosen about 30km.
The vertical profiles of temperature T(H) were retrieved from the Rayleigh and Raman signals using the formula

$$T(H) = \frac{P_1(H)P_2(H)}{N(H)H^2}\left[\frac{N(H_m)}{P_1(H_m)P_2(H_m)}T(H_m) + \frac{1}{R^*}\int_{H_m}^{H}\frac{N(h)h^2 g(h)dh}{P_1(h)P_2(h)}\right]$$

Here *N(H)* - lidar signals, *P1(H)* and *P2(H)* are the transparencies of the atmosphere from the level of arrangement of the lidar up to the height H at the wavelength of 532 nm (Rayleigh signals) and 532 and 607 nm (Raman signals), respectively; R^* is the universal gas constant, $g(h)$ is the gravity acceleration, *Hm* is the maximum height, from which quite reliable for processing signals are detected (so-called calibration height, at which the temperature values $T(Hm)$ are set).

3 RESULTS

3.1. Aerosol

The summary results of lidar observations of the stratospheric aerosol layer for the period 2016-18 are presented in Fig.1. In this picture measurements of the monthly mean dynamics of the aerosol vertical stratification are shown.

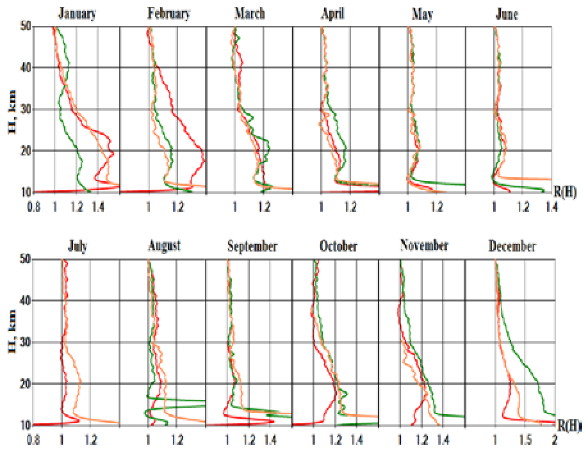

Fig. 1. Monthly mean profiles of the aerosol vertical stratification in 2016-2018. Red lines show the mean profiles in 2016, , green lines show the mean profiles in 2017, orange lines show the mean profiles in 2018.

The observations for this period of time indicate that the common feature for the region of the Western Siberia is the maximal aerosol loading of the stratosphere in winter months, almost no aerosol loading for the entire stratospheric layer in summer months, and no loading for the upper stratospheric layer from 30 to 50 km, except in winter months. Also, there are substantial differences in aerosol stratification. For instance, the aerosol loading was stronger in December 2017 as compared to 2016 and 2018, it was stronger in January 2016 and 2018, and stronger in February 2016.

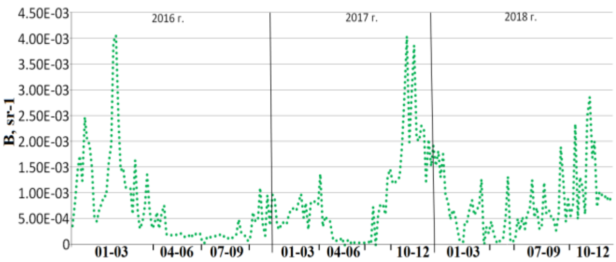

Fig.2 Time series of integrated aerosol backscattering coefficient for the period of 2016 – 2018.

Time dynamics of the total stratospheric loading with background aerosol in 2016-2018, expressed via a parameter of integrated aerosol backscattering coefficient, is presented in Fig. 2.

The observation time series, presented in Fig. 2, indicate a weak aerosol loading for cold period in November 2016 – April 2017 ($B(H) \leq 10^{-3}$sr^{-1}); quite a marked aerosol loading, strongly varying in time, for the period of January – April 2016; and a large aerosol loading for the period of October 2017 – February 2018 (up to $B(H) \approx 4 \cdot 10^{-3}$sr^{-1}). The aerosol loading was minimal in May – September 2016 and in May – August 2017. Abrupt bursts ($B(H) \geq 10^{-3}$sr^{-1}), and not only minima in aerosol content, were observed in spring, summer, and fall of 2018. The tendency of aerosol loading of the lower stratosphere, peaking in January, decreasing in spring, and almost vanishing in May – September, is confirmed by the comparison with observations in previous years [1,2].

3.2. Temperature.

Observations for January 2016 are presented in Fig. 1. In this figure, like in figures below, the vertical temperature profiles (VTP), obtained from lidar measurements, are compared with those, measured on Aura satellite [3] and at aerological sensing station in Novosibirsk [4], as well as those from CIRA-86 model [5].

From Fig. 3 it can be seen that the stratospheric warming (SW) began in the second decade of January, and continued on the next days of observations in a classical form of half-waves with a positive deviation from monthly average temperature in the upper half of the stratosphere and a negative deviation in its lower half.

The maximal positive deviation reached 40 K (January 12, altitude of 45 km), and maximal negative deviation was 35 K (January 5 and 7, altitude of about 30 km). From January 19 to 26, the vertical temperature distribution stabilized somewhat (approached the model distribution) in the upper stratosphere. However, in the entire layer of the lower atmosphere, the temperature profiles obtained from lidar, balloon, and satellite data remained shifted toward negative values relative to the model profile.

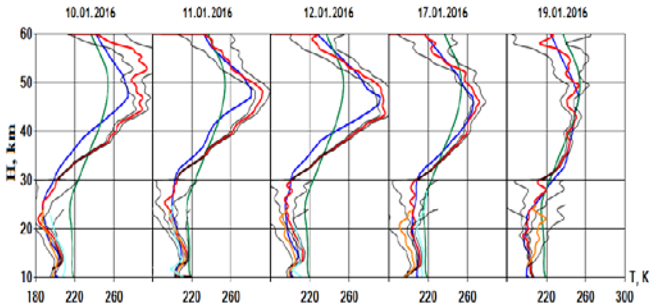

Fig. 3. Lidar and satellite observations of manifestation of stratospheric warming in January 2016. Temperature profiles, calculated from lidar measurements of Rayleigh and Raman signals (red and yellow lines) and their standard deviations (black lines), observations from Aura satellite and meteorological sondes (blue and light blue lines), and monthly average profile according to CIRA-86 model (green line).

The last overshoot of warming was observed on February 1 of 2016 in the height range of 40-60 km (see Fig.4). The analogous warming, but in the narrower height range of 45-60 km, was also observed from the data of satellite measurements. According to the data of the following observations, the final stage of stabilization of the vertical temperature distribution occurred. From Fig. 4, we can see that the temperature profiles obtained in the entire height range of 10-60 km from lidar, satellite, and balloon measurements become quantitatively and qualitatively closer to the model profile.

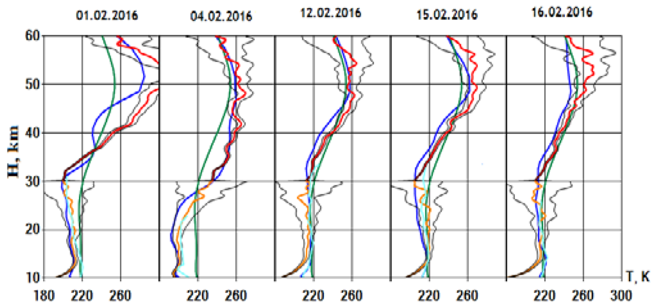

Fig. 4. Vertical distribution of temperature in some nights of February 2016.

The observed SW in 2016 was of the minor type, as indicated by the data taken from the website of the European center for medium-term weather forecasts [9].

Temperature profiles for the quiescent period of 2016 (from April to September) are shown in Fig. 5. In this long period of time, the stratosphere evolved into a stable thermal regime, in which the vertical temperature distribution well agrees with the monthly average model distribution.

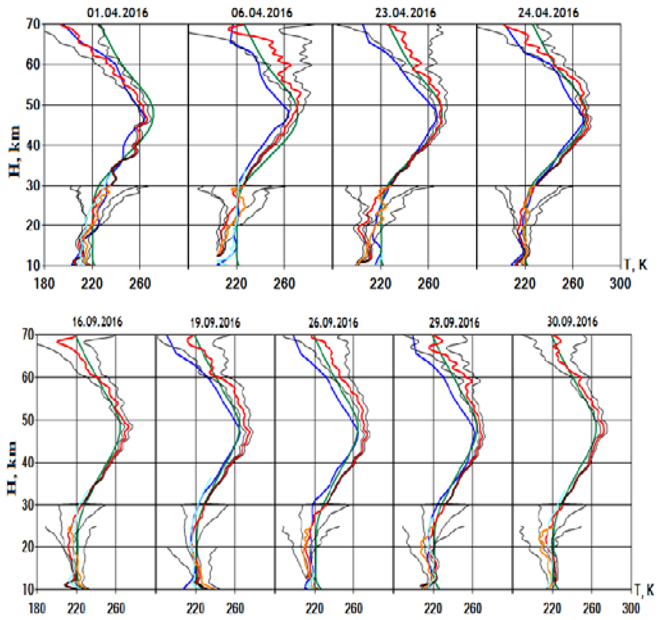

Fig. 5. Vertical temperature distribution on separate nights in April – September 2016.

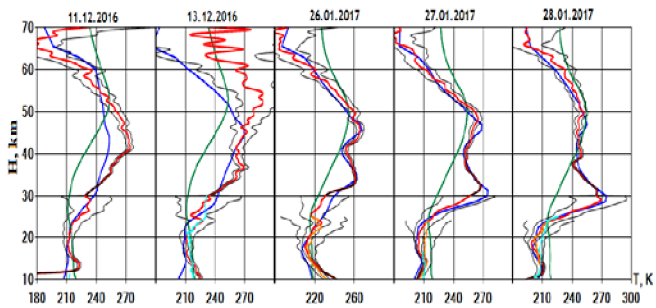

Fig. 6. Lidar and satellite observations of manifestation of stratospheric warming in winter 2016/2017.

The next stratospheric warming began in December (Fig. 6). For instance, on December 11 at the altitude of about 50 km there had been a positive deviation of temperature from monthly average by about 30 K. Then, the weather conditions were unfavorable, so that observations had been resumed as late as the end of January 2017. From Fig. 6 it can be seen that, as indicated by both lidar and satellite observations, the stratospheric warming continued for the third decade of January. It is noteworthy that the lidar and satellite measurements of temperature well agree. Based on these independent measurements, the warming pattern shows two peaks at altitudes of 30-32 and 47-50 km.

Then, in the next period of observations from February to December, the thermal regime of the stratosphere evolved into the stable state, indicated by a good correspondence between lidar/satellite and model-based temperature profiles (not shown).

Occurrence of stratospheric warming in winter 2017/2018 was recorded both by lidar and satellite measurements in the last decade of January 2018 (Fig. 7). The warming peaked in the stratopause region (January 21, H=50 km). On next days of observations, the stratopause altitude decreased to 40 km, and the maximal positive deviation reached 50 K.

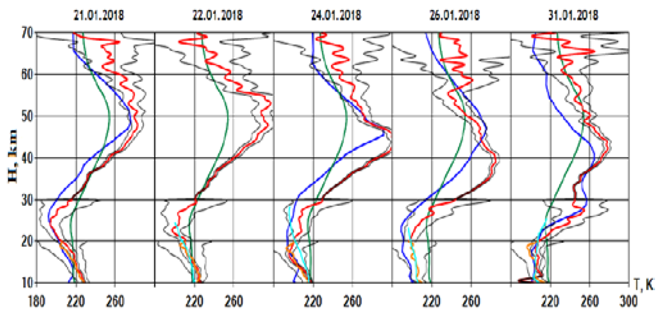

Fig.7. Lidar and satellite observations of manifestation of stratospheric warming in winter 2017/2018.

The vertical temperature distribution during the SW episode in December 2018 – January 2019 is shown in Fig. 8. A pronounced warming was localized at altitudes from 20 to 50 km, and was accompanied by a cooling at altitudes from 10 to 20 km. We note that the stratospheric warming was as long as the whole month and had a large (up to 60 K) amplitude of the positive deviation.

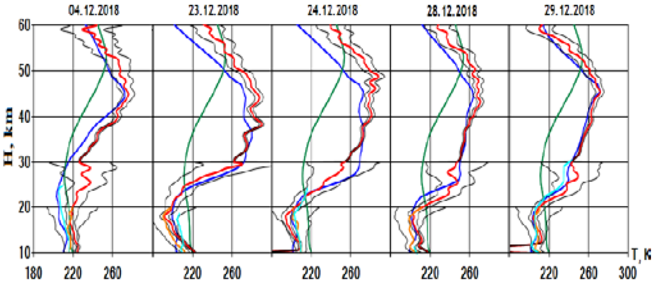

Fig. 8. Lidar and satellite observations of the dynamics of stratospheric warming during winter 2018/2019.

The SW in 2018-2019 was major in type, i.e., westerly air mass transport in the stratosphere reversed to easterly transport (see Fig. 9).

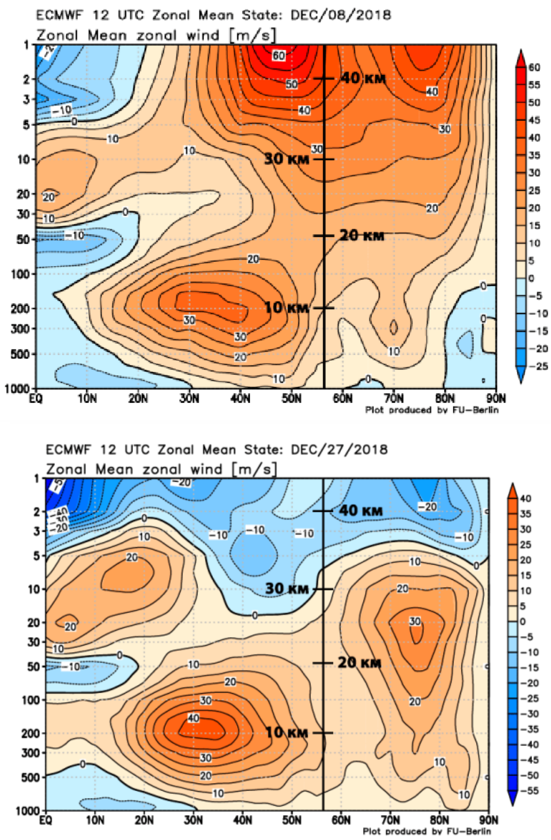

Fig. 9. Altitudinal distribution of zonal wind speed and direction in the Northern Hemisphere, recorded on December 8 and 27, 2018. Orange areas are for westerlies and blue areas for easterlies. The vertical thick lines indicate the altitudinal transects for the latitude of Tomsk.

CONCLUSION

The lidar studies of the stratosphere over Tomsk in the period of 2016-2018, as well as earlier years, revealed the following:

1. The loading of the stratosphere with background aerosol occurs in the cold period of a year: start in October, maximum in January, and end in April. In the warm period, there is practically no aerosol in the stratosphere.
2. Every year the winter warming takes place in the stratosphere. It begins in December, is most pronounced in January, and is sometimes extended to February. Weak and, more rarely, strong warmings are observed. The amplitude of positive temperature deviations from the monthly average value can achieve 60 K, and the height of the stratopause can go down to 30 km. In the period of March till November, the vertical temperature distribution is inasatisfactory agreement with the CIRA-86 model distribution.

This work was supported by the Russian Science Foundation (grant no. 19-7720067) in carrying out the monitoring measurements, and by the Russian Fund for Basic Research (project no. 19-45-700008) in the analysis of the lidar sensing data and the grant of President of RF MK-4592.2018.8

REFERENCES

[1] Marichev V.N. Investigation of variability of the background aerosol vertical structure above Tomsk based on lidar observations in 2010-2011, Atmos. Ocean Opt., 2012, 25. No. 11. P. 976-984.
[2] Marichev V.N., Bochkosvkii D.A. Studying the variations in background aerosol loading of the stratosphere in 2014, Proceedings of SPIE. 2015. V.9680. CID: 9680 6U. [9680-209]
[3] http://mirador.gsfc.nasa.gov
[4] http://weather.uwyo.edu/upperair/sounding.html
[5] Rees D., Barnett J.J., Labitske K. COSPAR International Reference Atmosphere: 1986. Part II, Middle Atmosphere Models // Adv. Space Res. 1990. V. 10, N 12. 525 p.
[6]http://users.met.fu-berlin.de/~Aktuell/strat-www/wdiag/eczm.php?alert=8&forecast=all&var=u&lng= eng#fig1
[7] Marichev V.N. Lidar investigations of stratospheric warming events above Tomsk in 2008-2010. // Atmos. Ocean Opt. 2011. V. 24. No. 05. pp. 386-391.
[8] Marichev V.N. Investigation into features of manifestation of winter stratospheric warming events over Tomsk from the data of lidar temperature measurements in 2010-2011. // Atmos. Ocean Opt. 2011. V. 24. No. 12. P. 1041-1046.
[9] Marichev V.N. The analysis of the air density and temperature behaviour in the stratosphere above Tomsk in periods of perturbed and quiet states performed according to the results of lidar measurements. // Atmos. Ocean Opt. 2013. V. 26. No. 09. pp. 783-792.